
Article:
Dimitri, P., Jacques, R.M., Paggiosi, M. et al. (6 more authors) (2014) Leptin may play a role in bone microstructural alterations in obese children. Journal of Clinical Endocrinology & Metabolism, 100 (2). 594 - 602.

https://doi.org/10.1210/jc.2014-3199

P Dimitri, RM Jacques, M Paggiosi, D King, J Walsh, ZA Taylor, AF Frangi, N Bishop, R Eastell. Leptin May Play a Role in Bone Microstructural Alterations in Obese Children. Journal of Clinical Endocrinology & Metabolism 2015; 100(2): 594-602.
doi: 10.1210/jc.2014-3199

Leptin may play a role in bone microstructural alterations in obese children

P. Dimitri[1], R. M. Jacques[2], M. Paggiosi[3], D. King[1], J. Walsh[3] Z.A. Taylor[4], A. F. Frangi[4], N. Bishop[3], R. Eastell[3]

1. The Department of Paediatric Endocrinology, Sheffield Children's NHS Foundation Trust, UK
2. School of Health and Related Research, University of Sheffield, Sheffield, UK
3. The Mellanby Centre for Bone Research, Academic Unit of Bone Metabolism, University of Sheffield, UK
4. Centre for Computational Imaging & Simulation Technologies in Biomedicine, The Department of Mechanical Engineering, University of Sheffield, UK

Abbreviated title: Leptin and bone microstructural change in obese children

Key terms: High resolution peripheral quantitative computed tomography; microfinite element analysis; skeletal microstructure; leptin; obesity

Corresponding author
Professor Paul Dimitri
The Department of Paediatric Endocrinology
Sheffield Children's NHS Foundation Trust
Western Bank
Sheffield, UK
S10 2TH
Phone: +44 114 271 7118
Email: paul.dimitri@sch.nhs.uk

Disclosures

All others authors have nothing to declare

Abstract

Context: Bone mass is low and fracture risk is higher in obese children. Hormonal changes in relation to skeletal microstructure and biomechanics have not been studied in obese children

Objective: To ascertain the relationships of obesity-related changes in hormones with skeletal microstructure and biomechanics.

Design: High resolution peripheral quantitative computed tomography (HR-pQCT) was used to compare 3-dimensional cortical and trabecular microstructure and biomechanics at load-bearing and non-load bearing sites in obese and lean children. The relationship between leptin, adiponectin, testosterone, estrogen, osteocalcin and sclerostin and skeletal microstructure was also determined.

Setting: Tertiary paediatric endocrine unit in the UK

Participants: Obese and lean children matched by gender and pubertal stage

Results: Radial cortical porosity (mean difference -0.01 [95% CI: -0.02, -0.004], p=0.003) and cortical pore diameter (mean difference -0.005mm [95% CI: -0.009, -0.001], p=0.011) were lower in obese children. Tibial trabecular thickness was lower (mean difference -0.009mm [95% CI: -0.014, -0.004], P=0.003) and trabecular number was higher (mean difference 0.23mm-1[95% CI: 0.08, 0.38], P=0.004) in obese children. At the radius, fat mass percentage negatively correlated with cortical porosity (r=-0.57, p<0.001) and pore diameter (r=-0.38, p=0.02) and negatively correlated with trabecular thickness (r=-0.62, p<0.001) and trabecular von Mises stress (r=-0.39, p=0.019) at the tibia. No difference was observed in the other biomechanical parameters of the radius and tibia.
Leptin was higher in obese children (805.3±440.6 vs 98.1±75.4, p<0.001) and was inversely related to radial cortical porosity (r=0.60, 95% CI:[-0.80, -0.30], p<0.001), radial cortical pore diameter (r=0.51, 95% CI[-0.75, -0.16], p=0.002), tibial trabecular thickness (r=0.55, 95% CI: [-0.78,-0.21], p=0.001) and tibial trabecular von Mises stress (r=-0.39, 95% CI: -0.65, 0.04, p=0.02).

Conclusion: Childhood obesity alters radial and tibial microstructure. Leptin may direct these changes. Despite this, the biomechanical properties of the radius and tibia do not adapt sufficiently in obese children to withstand the increased loading potential from a fall. This may explain the higher incidence of fracture in obese children.

Introduction

Epidemiological evidence suggests that the incidence of distal radius fractures has increased by 30% over the last 30 years (1). Concomitantly, there has been a significant increase in childhood obesity over the same period. To date, several studies have identified that overweight and obese children are over-represented in fracture groups (2–5) and that obesity may have a detrimental impact on skeletal development in children increasing bone fragility that may persist for several years (6–8). Other studies, however, point to a positive relationship between fat mass and bone size and mass during childhood and adolescence (9 –11). Alterations in adipokines such as leptin in obese children may be responsible for changes in local factors controlling osteoclastogenesis and bone modeling that predispose them to low bone mass and fracture (12).

High resolution peripheral quantitative computed tomography (CT) (HR-pQCT, isotropic voxel size 82 mm) provides the resolution required to accurately determine 3-dimensional in vivo bone microstructure at partially loaded (distal radius) and loaded (distal tibia) skeletal sites at a low radiation dose (<3 μSv per scan). At high resolution cortical porosity and pore diameter can also be determined from the images and may provide additional insight into the apparent bone fragility in children and adolescents (13). The application of microfinite element analysis to HR-pQCT images provides insight into the biomechanical properties of these skeletal sites. Alterations in skeletal microstructure and biomechanics identified by HR-pQCT during adolescence result in transient skeletal weakness in mid-puberty that coincides with the period of peak fracture incidence (14). The over-representation of overweight and obese children in fracture studies suggests that excess fat in children may alter skeletal microarchitecture or the biomechanical properties of bone that exacerbates this risk. In young adults visceral adipose tissue appears to have a detrimental effect on age-adjusted radial cortical volumetric density and trabecular thickness measured by HR-pQCT (15). To our knowledge, there are no studies that have directly assessed the impact of childhood obesity on bone microarchitecture and the biomechanical properties of bone using HR-pQCT. The aim of this study was to determine whether differences in cortical and trabecular bone microarchitecture and the biomechanical properties of the distal radius and tibia exist between obese and lean children matched for pubertal age and gender and whether changes in key hormones may explain these differences.

Materials and Methods

Study participants were divided into two groups according to Body Mass Index (BMI) percentile based upon the UK BMI Ref Reference Charts. Our study population consisted of 18 lean children (BMI < 91st percentile) and 18 obese participants (BMI > 98th percentile) matched for Tanner pubertal stage and gender (16). All participants were Caucasian and so ethnically matched. Participants were recruited from local advertisements and from healthy cohorts who had taken part in previous bone-related research. Obese participants were additionally recruited from the Pediatric

Endocrinology Clinic at Sheffield Children's Hospital, UK. The study was given ethical approval by South Yorkshire Research Ethics Committee. Written informed consent was obtained from all participants.

Participants underwent a structured history and examination. Pubertal stage was assessed either by direct examination by a Pediatric Endocrinologist or by the use of Tanner stage picture cards by which the subject identified their pubertal stage. Subjects were excluded if they had any of the following: fracture within the 12 months period prior to recruitment; previous orthopedic surgery or fractures, which preclude imaging at all sites; a history of any long term immobilization (duration greater than three months); diagnosed endocrine or chromosomal disorders; metabolic bone disease; chronic illness; restrictive eating disorders; use of depot medroxyprogesterone or the combined oral contraceptive (OC) pill or use of any steroid-based or other medications (including inhaled corticosteroids) known to alter bone metabolism. Previous fracture history was documented. This was then cross-referenced against radiographs and subsequent reports by senior radiologists to verify the region of fracture reported by the subjects.

Anthropometry was undertaken with the subjects wearing light clothing. Height was measured using a portable stadiometer (SECA 214 portable stadiometer, Birmingham, UK) to the nearest 1mm and weight to the nearest 0.1 kg using electronic balance scales (SECA 770 digital weighing scales, Birmingham, UK). Body Mass Index was calculated as weight (kg)/height (m^2). Height, weight and BMI SD score was calculated using the UK reference values produced by the Child Growth Foundation (17).

Total body BMD was acquired using the Discovery A densitometer (Hologic Inc., Bedford, MA, USA) and subtotal body fat (total body less head) (grams), truncal fat (grams) and subtotal lean mass (grams) were estimated from this. Device stability was monitored using an anthropomorphic spine phantom. Weekly scans of a European Spine Phantom (QRM—Quality Assurance in Radiology and Medicine, Moehrendorf, Germany) were also performed.

HR-pQCT image acquisition and analysis of the distal radius and tibia was performed using the standard built-in software (XtremeCT, version 6.0, Scanco Medical AG, Brüttisellen, Switzerland) and in accordance with the methods used previously by Paggiosi et al (38). In all post-pubertal participants with fused tibial and radial growth plates, a reference line was placed on the scan image at the endplate of the distal tibia and on the notch on the articular surface of the distal radius to indicate the position of the first measurement slice (22.5 mm and 9.5 mm proximal from the reference line for the tibia and radius respectively). In pre-pubertal and those participants with open tibial and

radial growth plates, the reference line was placed on the scan image at the proximal end of the growth plate to indicate the position of the first measurement slice (1 mm proximal from the reference line) (18). All scans were performed using the non-dominant limb. A single stack of parallel CT slices (110 slices = 9.02 mm) for each site was acquired in the high resolution mode (image matrix = 1536 × 1536). Daily measurements of the manufacturer device-specific phantom (Scanco Medical AG, Brüttisellen, Switzerland) were performed to monitor the stability of the XtremeCT.

HR-pQCT densitometric measurements included total density (D_{tot}, milligrams per cubic centimeter), trabecular density (D_{trab}, milligrams per cubic centimeter), and cortical density (D_{cort}, milligrams per cubic centimeter). Measures of microstructural properties included trabecular number (Tb.N, 1/millimeters), trabecular thickness (Tb.Th, millimeters), trabecular separation (Tb.Sp, millimeters), bone volume fraction (BV/TV, percent), and cortical thickness (Ct.Th, millimeters). Extended cortical bone analysis techniques were applied to the segmented scans using specialist software provided by Scanco Medical AG (version 6) and following the approaches described by Burghardt et al (19, 20) and Nishiyama et al (21) to assess cortical porosity (Ct.Po, percent) and mean cortical pore diameter (Ct.Po.Dm, micrometers).

Measures of bone strength were determined by microfinite element analysis (mFEA) using software developed by Scanco Medical AG (version 1.13; FE-solver included in the Image Processing Language) (22). Segmented images were automatically converted into micro-FE models, in which each voxel of bone material becomes a single hexahedral finite element. Such models allow tissue-level stresses and strains to be computed directly, potentially providing a more reliable estimate of the mechanical environment within the distal radius and tibia. Analysis results were post processed to derive various measures of overall specimen stiffness and strength. Models of the radial and tibial specimens undergoing quasi-static axial (ie, along the long axes of the bones) compression were used (23). Analysis variables included bone stiffness (S, kilonewtons per millimeter), estimated ultimate failure load (F.ult, kilonewtons), the ratio of the load taken by the trabecular bone in relation to the total load at the distal end ($Tb.F/TF_{dist}$, percent) and proximal end ($Tb.F/TF_{prox}$, percent), and average von Mises stresses in the trabecular (Tb.VM, megapascals) and the cortical (C.VM, megapascals) bone. Von Mises stress (σ_v) is a convenient scalar measure of stress intensity at a given point. It is calculated from the von Mises criterion, a formula for calculating the stress combination across three principle axes (x,y,z). The individual axial stress may not exceed the yield stress, but yielding or fracture may occur through a combination of stresses. The von Mises criterion is a formula for combining these 3 stresses into an equivalent stress (von Mises stress), which is then compared to the yield or failure stress of the material (σ_y). If the von Mises Stress exceeds the yield stress, then the material will fail. Bone Strength Index (BSI) was calculated for the distal radius and tibia. The BSI as

a surrogate for compressive bone strength was calculated using D_{tot} and $Area_{tot}$: [$BSI(mg^2/mm^4) = D_{tot}^2 \times Area_{tot}$] (24).

Venous blood sampling was performed at 09:00am to avoid diurnal variation in metabolic profiles. Serum was analyzed for leptin, adiponectin, testosterone, estradiol, osteocalcin and the osteoblast inhibitor sclerostin. The Cobas e411 automated immunoassay (Roche Diagnostics, Germany) was used to measure teststosterone (interassay coefficient of variation (CV) 2.6%, intra-assay CV 1.7%), estradiol (interassay CV 5.4%, CV 1.4%) and osteocalcin (interassay-CV 2.2%, intra-assay CV 1.8%). Leptin (interassay CV 3.8%, intra-assay CV 3.1%) and adiponectin (interassay CV 2.8%, intra-assay CV 3.0%) were measured using the Quantikine ELISA (R&D Systems Europe, Ltd, United Kingdom). Sclerostin (interassay CV 5.4%, intra-assay CV 3.0%) was measured by ELISA (Biomedica Gruppe, Austria).

Statistical Analysis

Paired t-tests were used to make comparisons of age, anthropometry, HR-pQCT bone parameters and measures of bone strength between lean and obese pairs matched for gender and puberty. In addition, to account for body size, analysis of covariance (ANCOVA) with matched pair as a random effect was used to adjust the differences in HR-pQCT and measures of bone strength between lean and obese groups for height. Weight was not adjusted for in the ANCOVA model because of colinearity with the categorical variable identifying lean and obese (ie, the variables are highly correlated). Similarly, paired t-tests were used to compare differences in serum values of biochemical parameters between obese and lean children. The associations between HR-pQCT variables and measures of bone strength with body composition and biochemical measures were assessed by Spearman rank correlations with 95% confidence intervals calculated using bootstrapping. Multivariate analysis was subsequently used to determine the relationship between biochemical profiles and relevant skeletal microstructural parameters. All statistical analyses were undertaken in SPSS Statistics for Windows, Version 21 (IBM Corp., Armonk, NY, USA). Graphs were produced using R Version 3.0.2 (R Foundation for Statistical Computing, Vienna, Austria). Significance was determined at a p-value of less than or equal to 0.05.

Results

Participant characteristics

There was no significant difference in mean decimal age and height SDS between the lean and obese groups (Table 1). In addition to the expected difference in BMI SDS and fat mass, lean mass was significantly greater in the obese group. In the lean group, 11% (2/18) children had previously fractured compared with 33% (6/18) children in the obese group. All but one child had sustained an upper limb fracture.

Comparison of bone microarchitecture and strength between obese and lean groups

There was a 1.27 (95% CI: 0.49 to 2.06, P = .003) standard deviation difference in cortical porosity between groups at the distal radius and cortical pore diameter was 1.05 (95% CI: 0.27 to 1.84, P = .011) and 0.62 (95% CI: 0.16 to 1.08, P = .012) standard deviations lower at the distal radius and tibia respectively in the obese group (Table 2). No difference in trabecular microstructure was identified at the radius. In contrast, mean tibial trabecular thickness and tibial trabecular separation was 1.01 (95% CI: 0.41 to 1.61, P=.003) standard deviations lower and tibial trabecular number was 0.74 (95% CI: 0.27 to 1.22, P =.004) standard deviations higher in the obese group (table 2, figure 1a). Mean tibial cortical pore diameter was significantly lower in obese children although there was no difference identified in the degree of cortical porosity (Table 2, figure 1a).

Average von Mises stress in the trabecular bone was significantly lower in obese children (unadjusted mean difference –0.31mPA, 95% CI: –0.62, –0.001, P = .049) although this relationship lost significance when adjusting for height (mean difference –0.31mPA, 95% CI: –0.63, 0.01, P=.058). There were no other differences identified in the microfinite element parameters between lean and obese groups at the radius and tibia (Table 3 and figure 1b).

Correlation with subtotal body and truncal fat and subtotal body lean mass was determined for cortical and trabecular microstructure and strength parameters that were previously identified as being significantly different between lean and obese groups (Table 4). Subtotal and truncal fat mass had the strongest association with cortical porosity and mean cortical pore diameter at the radius and trabecular thickness at the distal tibia. Total body (r=- 0.39, 95% CI: -0.68, -0.03, P=.019) and truncal mass (r=-0.37, 95% CI: -0.62, -0.07, P =.028) was inversely associated with tibial trabecular von Mises stress.

Biochemistry Results

Serum leptin was significantly higher in obese children (Table 5). However, there was no difference in other biochemical/hormonal levels between groups.

As we only identified a difference in leptin between the two groups, we wished to determine the relationship between leptin and bone microstructural and strength parameters that may help to explain the differences in skeletal microstructure and strength between lean and obese children. At the radius, there was a strong inverse correlation between leptin and cortical porosity (r=-0.60, 95% CI: -0.80, –0.30, P < .001), mean cortical pore diameter (r=-0.51, 95% CI: –0.75, –0.16, P = .002) and a weaker inverse correlation with trabecular thickness (r=- 0.35, 95% CI: -0.63, –0.04, P = .037). There was no relationship between leptin and microFE parameters at the radius. At the tibia, leptin was inversely correlated with trabecular thickness (r=-0.55, 95% CI: -0.78, –0.21, P =.001) and tibial trabecular von

Mises stress (r=-0.39, 95% CI: -0.65, 0.04, P= .02). In multivariate analyses (multiple regression) that included all measured biochemical and hormonal factors, leptin remained inversely correlated to radial cortical porosity (r^2=0.56, P = .02), mean radial cortical pore diameter (r^2=0.29, P=.01) and tibial trabecular thickness (r^2=0.23, P= .02).

Discussion

Despite a higher lean mass and fat mass observed in the obese group, the only difference observed in radial microstructure was a reduction in cortical porosity and mean cortical pore diameter in the obese group. This change was more likely to be due to an increased fat rather than lean mass. Although ex vivo studies have demonstrated that greater cortical porosity results in lower bone strength (25, 26), previous in vivo pQCT analysis in children demonstrates that cortical area and volumetric BMD are more important determinants of resistance to fracture in the presence of compressive forces (27). No difference in cortical area and volumetric BMD was observed between groups and a greater number of children in our obese group had previously sustained a fracture, all of which were in the upper limb in keeping with previous studies (2, 28). We also observed no difference ultimate failure load, bone stiffness or bone strength index (BSI) between groups at the radius between the obese and lean cohorts. Bone stiffness refers to the extent to which bone resists deformation in response to an applied force. Ultimate failure load (F.ult) was computed as the applied load on the specimen that would result in 2% or more of the bone tissue exceeding its yield strain value (23). As such, it is a direct measure of bone strength at the organ-level, on the basis of which different individuals may be compared. A previous study using a rheological-stochastic model of arm impact incorporating anthropometric and DXA data demonstrated that obese children were at 1.7 greater risk of fracture compared to non-obese children. Lower fall heights and softer impact surfaces did not reduce this risk (29). Obese children were found to be at a greater risk of fracture as bodyweight is transmitted through the forearm during a fall particularly at lower impact heights when bodyweight contributes to a significant portion of the force of impact. We therefore speculate that the increase risk of fracture in obese children may result from the greater force from the fall exceeding the ultimate failure load of the distal radius due to a failure in the radius to adapt appropriately to increased fat and lean mass in obese children (30).

At the tibia, a fully loaded skeletal site, there was no difference in the cortical parameters between lean and obese pairs despite the higher lean mass and an increased load bearing through greater body weight on the lower limbs in obese children. Our findings are, however, not consistent with others who have demonstrated higher tibial cortical area and density in obese children (31, 32) and a positive effect of lean mass on bone density (10). In contrast, the novel finding in this study was that trabecular organization was different between groups, with obese children having a greater number and more closely spaced trabeculae due to an increase in fat mass. This may reflect the reduction in

von Mises stress in obese children. However, average rather than peak values for cortical and trabecular von Mises stress were derived from the HR-pQCT microFE analysis. Therefore, the lower average von Mises stress in the obese group cannot be used to infer fracture risk; thus this variable must be viewed with caution. Moreover, although the average tibial trabecular von Misesstress was lower in obese children (P = .049), no differences between groups were found in tibial cortical, radial cortical, or radial trabecular average values. These small differences in average von Mises stress suggest a similar overall pattern to that concluded from the estimates for the ultimate failure load (F.ult) ie, there is no adaptation in the biomechanical properties of the radius or tibia in obese children. Whereas ultimate failure load relates directly to material failure, the average von Mises stress does not; in terms of fracture likelihood, therefore, the former is a more informative measure for comparing the two groups. As there was no difference in ultimate failure load or BSI at the tibia between groups, we conclude that despite the change in tibial trabecular microarchitecture, there is insufficient biomechanical adaptation in the tibiae to withstand the increase in force that would occur from excessive body weight during a fall or twisting, thus explaining the increase in lower limb fractures observed in obese children (5). As cortical area and volumetric BMD appear to be more important determinants of forearm fracture in children (27) we suggest that it may be the failure of these elements to change in the tibia of obese children that results in an increased risk of fracture in combination with a greater risk of falling (33).

As expected, serum leptin was significantly higher in obese children. Leptin had a strong relationship with cortical porosity at the radius and mean trabecular thickness at the tibia as demonstrated in multivariate analysis with other key hormones. We, therefore hypothesize that leptin may be contribute to the radial and tibial microstructural change observed in obese children during skeletal development. We are the first group to report an association between leptin and an obesity-related reduction in radial cortical porosity and tibial trabecular thickness in children. While this does not support a pathomechanistic relationship, evidence from animal models provides some support for these findings. In growing mice with dietary induced obesity, lower tibial trabecular thickness, number, bone volume and density have been observed is separate studies during skeletal development (34, 35) associated with increased serum leptin rather than adiponectin and insulin (34). Mice treated with a leptin antagonist show an increase in lumbar trabecular thickness and number at 12 weeks suggesting that elevated leptin may impact on the developing skeleton (36). Increased trabecular number and bone volume in the long bones of 6-month-old leptin deficient (ob/ob) and leptin receptor– deficient (db/db) mice has been reported (37) although others have demonstrated a reduction in trabecular number and thickness in db/db mice (38). Leptin deficiency in mice impacts on cortical bone resulting in a reduction in cortical thickness supporting a positive effect of leptin on cortical bone (37, 39). In contrast others have shown a negative correlation between tibial cortical thickness, cross-sectional area and leptin in young adult males (40).

The level of circulating leptin in children may be relevant to the impact of childhood obesity on skeletal microarchitecture. Mean serum leptin was over eight times higher in our obese group. Whereas studies have demonstrated that leptin promotes the production of the osteoclastogenic inhibitor - osteoprotegerin (OPG) by osteoblast lineage cells, others have shown that higher concentrations of leptin (ten-fold greater than those optimal for OPG production) are associated with inhibition of OPG and receptor activator of nuclear factor kappa-B ligand (RANKL) production by osteoblasts (41). In vivo support for this finding comes from studies in tail-suspended rats, where lower doses of leptin appear to be protective of bone loss, but higher doses increase bone loss by increasing bone resorption and reducing bone formation (42). Leptin deficient mice have a high bone mass phenotype that can be recovered by cerebral intraventricular injection of leptin resulting in a loss of trabecular bone (37). Support for leptin acting as a key hormone altering skeletal development in obese children also comes from studies in children with profound changes in body composition. Children with congenital leptin deficiency are profoundly overweight yet they appear to have normal age and gender related whole body bone mineral content and density despite being hypogonadal and having hyperparathyroidism (43, 44) suggesting that severe leptin deficiency is bone protective in these children.

Limitations

Differences in bone microarchitecture relative to pubertal stage and gender have been previously described (46). By matching obese and lean children by pubertal stage and gender, we aimed to eliminate these differences sufficiently to detect differences in cortical and trabecular microarchitecture between lean and obese children and to determine the effects of fat and lean mass on the size of these differences. The primary limitation of this study was the number of participants despite matching. We are aware that the comparison of skeletal microarchitecture and strength between obese and lean adolescents may yield results that are indicative of changes at the distal radius and tibia, but a larger scale study is required to support these findings. While matching by pubertal stage attempts to address the impact of physiological maturity on bone, this may not be sufficient to address more subtle physiological differences that may result in skeletal maturation. However, as obese children enter puberty at an earlier stage, we would have expected differences in skeletal microstructure reflecting greater maturity. We recognize that physical activity levels may influence bone modelling and remodelling in children; physical activity was not measured in this study. Further work is required to determine whether the loads generated in relation to body weight from a fall are sufficient to cause fracture based upon the biomechanical properties of the radius and tibia relative to compressive, tensile and bending forces. As leptin is exclusively produced by adipocytes, we recognize that leptin may also be acting as a proxy for other adipogenic factors that may alter skeletal microarchitecture. Other cytokines and hormonal factors in addition to those

measured may also contribute to the skeletal differences observed between lean and obese children and require further study in the future.

Summary

Leptin may play a role in altering the microstructural properties of the cortex of the radii and trabecular bone of the tibiae in obese children. However, these alterations do not alter the potential of either of these bones to withstand greater loading. This may increase the propensity to fracture in obese children due to increased loading from the force generated from greater body weight during a fall.

Acknowledgements

I would like to thank Selina Bratherton for carrying out skeletal imaging, James Bull and Susan Lenthall for sample collection and Fatma Gossiel for sample analysis.

References

1. Khosla, S., Melton, L.J., III, Dekutoski, M.B., Achenbach, S.J., Oberg, A.L., and Riggs, B.L. Incidence of Childhood Distal Forearm Fractures Over 30 Years: A Population-Based Study. Journal of the American Medical Association. 2003;290:1479–1485.

2. Goulding, A., Grant, A.M., and Williams, S.M. Bone and Body Composition of Children and Adolescents With Repeated Forearm Fractures. J Bone Miner Res. 2005;20:2090–2096.

3. Manias, K., McCabe, D., and Bishop, N. Fractures and recurrent fractures in children; varying effects of environmental factors as well as bone size and mass. Bone. 2006;39:652–657.

4. Fornari, E.D., Suszter, M., Roocroft, J., Bastrom, T., Edmonds, E.W., and Schlechter, J. Childhood obesity as a risk factor for lateral condyle fractures over supracondylar humerus fractures. Clin Orthop Relat Res. 2013;471:1193–1198.

5. Kessler, J., Koebnick, C., Smith, N., and Adams, A. Childhood obesity is associated with increased risk of most lower extremity fractures. Clin Orthop Relat Res. 2013;471:1199–1207.

6. Cole, Z.A., Harvey, NC, Kim, M., Ntani, G., Robinson, S.M., Inskip, H.M., Godfrey, K.M., Cooper, C., and Dennison, E.M. Increased fat mass is associated with increased bone size but reduced volumetric density in pre pubertal children. Bone. 2012;50:562–567.

7. Farr, J.N., Chen, Z., Lisse, J.R., Lohman, T.G., and Going, S.B. Relationship of total body fat mass to weight-bearing bone volumetric density, geometry, and strength in young girls. Bone. 2010; 46:977–984.

8. Dimitri, P., Bishop, N., Walsh, J.S., and Eastell, R. Obesity is a risk factor for fracture in children but is protective against fracture in adults: a paradox. Bone. 2012;50(2):457–66.

9. Crabtree, NJ, Kibirige, M.S., Fordham, J.N., Banks, L.M., Muntoni, F., Chinn, D., Boivin, C.M., and Shaw, NJ. The relationship between lean body mass and bone mineral content in paediatric health and disease. Bone. 2004;35:965–972.

10. Leonard, M.B., Shults, J., Wilson, B.A., Tershakovec, A.M., and Zemel, B.S. Obesity during childhood and adolescence augments bone mass and bone dimensions. American journal of clinical nutrition. 2004;80:514–523.

11. Clark, E.M., Ness, A.R., Tobias, J.H., and and the Avon Longitudinal Study of Parents and Children Study, T. Adipose Tissue Stimulates Bone Growth in Prepubertal Children. Journal of clinical endocrinology and metabolism. 2006;91:2534–2541.

12. Dimitri, P., Wales, J.K., and Bishop, N. Adipokines, bone-derived factors and bone turnover in obese children; evidence for altered fat-bone signalling resulting in reduced bone mass. Bone;. 2011; 48(2):189 –96.

13. Farr, J.N., Amin, S., Melton, L.J., 3rd, Kirmani, S., McCready, L.K., Atkinson, E.J., Muller, R., and Khosla, S. Bone strength and structural deficits in children and adolescents with a distal forearm fracture resulting from mild trauma. J Bone Miner Res. 2014;

14. Nishiyama, K.K., Macdonald, H.M., Moore, S.A., Fung, T., Boyd, S.K., and McKay, H.A. Cortical porosity is higher in boys compared with girls at the distal radius and distal tibia during pubertal growth: an HR-pQCT study. J Bone Miner Res. 2012;27:273–282.

15. Ng, A.C., Melton, L.J., 3rd, Atkinson, E.J., Achenbach, S.J., Holets, M.F., Peterson, J.M., Khosla, S., and Drake, M.T. Relationship of adiposity to bone volumetric density and microstructure in men and women across the adult lifespan. Bone. 2013;55:119–125.

16. Cole, T.J., Freeman, J.V., and Preece, M.A. Body mass index reference curves for the UK, 1990. Archives of disease in childhood. 1995;73:25–29.

17. Child Growth Foundation.BMIcharts.UKcross-sectional reference data: 1990/1. Child Growth Foundation, 2 Mayfield Avenue, London W4 1PW.

18. Paggiosi, M.A., Eastell, R., and Walsh, J.S. Precision of high-resolution peripheral quantitative computed tomography measurement variables: influence of gender, examination site, and age. Calcif Tissue Int. 2014;94:191–201.

19. Burghardt, A.J., Buie, H.R., Laib, A., Majumdar, S., and Boyd, S.K. Reproducibility of direct quantitative measures of cortical bone microarchitecture of the distal radius and tibia by HR-pQCT. Bone. 2010;47:519–528.

20. Engelke, K., Stampa, B., Timm, W., Dardzinski, B., de Papp, A.E., Genant, H.K., and Fuerst, T. Short-term in vivo precision of BMD and parameters of trabecular architecture at the distal forearm and tibia. Osteoporos Int. 2012;23:2151–2158.

21. Nishiyama, K.K., Macdonald, H.M., Buie, H.R., Hanley, D.A., and Boyd, S.K. Postmenopausal women with osteopenia have higher cortical porosity and thinner cortices at the distal radius and tibia Than women with normal aBMD: an in vivo HR-pQCT study. J Bone Miner Res. 2010;25:882–890.

22. Boutroy, S., Van Rietbergen, B., Sornay-Rendu, E., Munoz, F., Bouxsein, M.L., and Delmas, P.D. Finite element analysis based on in vivo HR-pQCT images of the distal radius is associated with wrist fracture in postmenopausal women. J Bone Miner Res. 2008;23: 392–399.

23. Pistoia, W., van Rietbergen, B., Lochmuller, E.M., Lill, C.A., Eckstein, F., and Ruegsegger, P. Estimation of distal radius failure load with micro-finite element analysis models based on three-dimensional peripheral quantitative computed tomography images. Bone. 2002;30:842–848.

24. Kontulainen, S.A., Johnston, J.D., Liu, D., Leung, C., Oxland, T.R., and McKay, H.A. Strength indices from pQCT imaging predict up to 85% of variance in bone failure properties at tibial epiphysis and diaphysis. J Musculoskelet Neuronal Interact. 2008;8:401–409.

25. Wachter, NJ, Augat, P., Krischak, G.D., Mentzel, M., Kinzl, L., and Claes, L. Prediction of cortical bone porosity in vitro by microcomputed tomography. Calcif Tissue Int. 2001;68:38–42.

26. Yeni, Y.N., Brown, C.U., Wang, Z., and Norman, T.L. The influence of bone morphology on fracture toughness of the human femur and tibia. Bone. 1997;21:453–459.

27. Kalkwarf, H.J., Laor, T., and Bean, J.A. Fracture risk in children with a forearm injury is associated with volumetric bone density and cortical area (by peripheral QCT) and areal bone density (by DXA). Osteoporos Int. 2011;22:607–616.

28. Valerio, G., Galle, F., Mancusi, C., Di Onofrio, V., Guida, P., Tramontano, A., Ruotolo, E., and Liguori, G. Prevalence of overweight in children with bone fractures: a case control study. BMC Pediatr. 22;. 2012;12:166.

29. Davidson, P.L., Goulding, A., and Chalmers, D.J. Biomechanical analysis of arm fracture in obese boys. J Paediatr Child Health. 2003;39:657–664.

30. Farr, J.N., Amin, S., Melton, L.J., 3rd, Kirmani, S., McCready, L.K., Atkinson, E.J., Muller, R., and Khosla, S. Bone strength and structural deficits in children and adolescents with a distal forearm fracture due to mild trauma. J Bone Miner Res. 2014;29(3):590–9.

31. Vandewalle, S., Taes, Y., Van Helvoirt, M., Debode, P., Herregods, N., Ernst, C., Roef, G., Van Caenegem, E., Roggen, I., Verhelle, F., et al. Bone size and bone strength are increased in obese male adolescents. J Clin Endocrinol Metab. 2013;98:3019–3028.

32. Wetzsteon, R.J., Petit, M.A., Macdonald, H.M., Hughes, J.M., Beck, T.J., and McKay, H.A. Bone structure and volumetric BMD in overweight children: a longitudinal study. J Bone Miner Res. 2008;23:1946–1953.

33. Goulding, A., Jones, I.E., Taylor, R.W., Piggot, J.M., and Taylor, D. Dynamic and static tests of balance and postural sway in boys: effects of previous wrist bone fractures and high adiposity. Gait Posture. 2003;17:136–141.

34. Fujita, Y., Watanabe, K., and Maki, K. Serum leptin levels negatively correlate with trabecular bone mineral density in high-fat diet-induced obesity mice. J Musculoskelet Neuronal Interact. 2012;12: 84–94.

35. Cao, J.J., Gregoire, B.R., and Gao, H. High-fat diet decreases cancellous bone mass but has no effect on cortical bone mass in the tibia in mice. Bone. 2009;44:1097–1104.

36. Solomon, G., Atkins, A., Shahar, R., Gertler, A., and Monsonego- Ornan, E. Effect of peripherally administered leptin antagonist on whole body metabolism and bone microarchitecture and biomechanical properties in the mouse. Am J Physiol Endocrinol Metab. 2014;306:E14–27.

37. Ducy, P., Amling, M., Takeda, S., Priemel, M., Schilling, A.F., Beil, F.T., Shen, J., Vinson, C., Rueger, J.M., and Karsenty, G. Leptin inhibits bone formation through a hypothalamic relay: a central control of bone mass. Cell. 2000;100:197–207.

38. Williams, G.A., Callon, K.E., Watson, M., Costa, J.L., Ding, Y., Dickinson, M., Wang, Y., Naot, D., Reid, I.R., and Cornish, J. Skeletal phenotype of the leptin receptor-deficient db/db mouse. J Bone Miner Res. 2011;26:1698–1709.

39. Hamrick, M.W., Pennington, C., Newton, D., Xie, D., and Isales, C. Leptin deficiency produces contrasting phenotypes in bones of the limb and spine. Bone. 2004;34:376–383.

40. Lorentzon, M., Landin, K., Mellstrom, D., and Ohlsson, C. Leptin is a negative independent predictor of areal BMD and cortical bone size in young adult Swedish men. J Bone Miner Res. 2006;21:1871– 1878.

41. Lamghari, M., Tavares, L., Camboa, N., and Barbosa, M.A. Leptin effect on RANKL and OPG expression in MC3T3–E1 osteoblasts. J Cell Biochem. 2006;98:1123–1129.

42. Martin, A., David, V., Malaval, L., Lafage-Proust, M.H., Vico, L., and Thomas, T. Opposite effects of leptin on bone metabolism: a dose-dependent balance related to energy intake and insulin-like growth factor-I pathway. Endocrinology. 2007;148:3419–3425.

43. Farooqi, I.S., Jebb, S.A., Langmack, G., Lawrence, E., Cheetham, C.H., Prentice, A.M., Hughes, I.A., McCamish, M.A., and O'Rahilly, S. Effects of Recombinant Leptin Therapy in a Child with Congenital Leptin Deficiency. New England journal of medicine. 1999;341:879–884.

44. Montague, C.T., Farooqi, I.S., Whitehead, J.P., Soos, M.A., Rau, H., Wareham, NJ, Sewter, C.P., Digby, J.E., Mohammed, S.N., Hurst, J.A., et al. Congenital leptin deficiency is associated with severe early-onset obesity in humans. Nature. 1997;387:903–908.

45. Ohwada, R., Hotta, M., Sato, K., Shibasaki, T., and Takano, K. The relationship between serum levels of estradiol and osteoprotegerin in patients with anorexia nervosa. Endocrine journal. 2007;54:953– 959. .

46. Burrows, M., Liu, D., and McKay, H. High-resolution peripheral QCT imaging of bone micro-structure in adolescents. Osteoporos Int. 2010;21:515–520.

Figure 1: Difference in mean and standard deviation score for **(a)** cortical and trabecular bone microstructure parameters **(b)** for HR-pQCT derived microFE bone strength, for lean and obese groups. Values are standardized using the mean and SD from the lean group. Circles represent the mean and lines represent the 95% confidence intervals

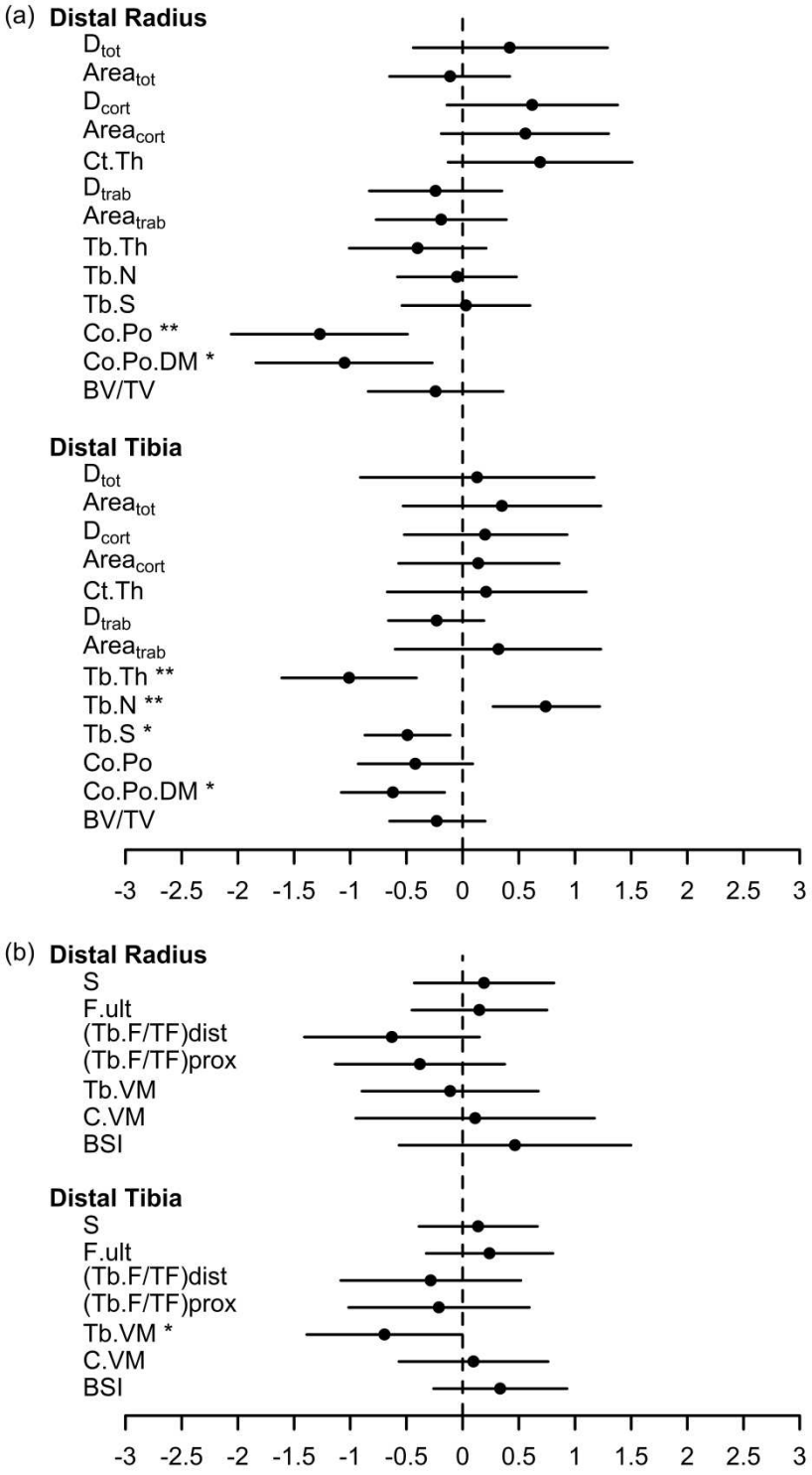

Table 1: Comparison of anthropometry in lean and obese groups and mean difference (95% confidence interval) matched by gender and pubertal stage. Significance is reached at p≤0.05

	Lean (n = 18) Mean (SD)	Obese (n = 18) Mean (SD)	Mean Difference (95% CI)	P-Value
Age (years)	12.9 (2.0)	12.6 (1.9)	-0.3 (-0.8, 0.2)	0.229
Height SDS	1.12 (1.34)	0.96 (1.41)	-0.16 (-0.96, 0.63)	0.667
Weight SDS	0.55 (0.92)	3.19 (0.87)	2.64 (2.20, 2.99)	<0.001
BMI SDS	0.08 (0.87)	3.14 (0.68)	3.06 (2.68, 3.44)	<0.001
Lean mass (grams)	33129 (9084)	43115 (11166)	9986 (6404, 13568)	<0.001
Subtotal fat mass (grams)	11935 (5133)	38706 (14447)	26771 (20474, 33068)	<0.001
Subtotal percentage fat mass (%)	26.3 (7.5)	46.6 (5.3)	20.3 (16.5, 24.1)	<0.001
Truncal fat mass (grams)	4767 (2307)	17538 (7441)	12772 (9627, 15916)	<0.001
Truncal percentage fat mass (%)	21.4 (6.6)	43.2 (6.0)	21.8 (18.5, 25.2)	<0.001

Table 2: Comparison of HR-pQCT cortical and trabecular parameters between obese and lean children matched for pubertal stage and gender calculated by paired t-tests and ANCOVA (The adjustment was for height as a covariate in the analysis). Significance is reached at p≤0.05

DISTAL RADIUS						
HRpQCT parameter	Lean (n=18) Mean (SD)	Obese (n=18) Mean (SD)	Unadjusted* Mean Difference (95% CI)	P-Value	Adjusted** Mean Difference (95% CI)	P-Value
D_{tot} (mg/cm^3)	253.3 (33.5)	267.5 (40.6)	14.2 (-14.6, 43.1)	0.313	13.8 (-15.5, 43.2)	0.333
$Area_{tot}$(mm^2)	237.8 (53.8)	231.7 (64.7)	-6.1 (-35.0, 22.8)	0.662	-5.2 (-32.1, 21.7)	0.688
D_{cort}(mg/cm^3)	687.5 (50.4)	718.6 (71.6)	31.1 (-7.1, 69.3)	0.104	30.8 (-8.6, 70.3)	0.117
$Area_{cort}$(mm^2)	27.3 (8.6)	32.1 (11.8)	4.8 (-1.6, 11.2)	0.134	4.8 (-1.8, 11.4)	0.144
Ct.Th (mm)	0.44 (0.14)	0.54 (0.20)	0.10 (-0.02, 0.21)	0.095	0.10 (-0.02, 0.22)	0.107
D_{trab}(mg/cm^3)	170.0 (29.4)	163.0 (25.8)	-7.0 (-24.3, 10.3)	0.404	-7.2 (-25.0, 10.6)	0.405
$Area_{trab}$(mm^2)	201.0 (50.6)	191.5 (63.3)	-9.5 (-38.7, 19.7)	0.501	-8.7 (-36.3, 19.0)	0.516
Tb.Th (mm)	0.066 (0.006)	0.064 (0.009)	-0.002 (-0.006, 0.001)	0.188	-0.002 (-0.006, 0.001)	0.198
Tb.N (mm^{-1})	2.15 (0.27)	2.13 (0.21)	-0.01 (-0.16, 0.13)	0.847	-0.02 (-0.16, 0.13)	0.828
Tb.S (mm)	0.41 (0.06)	0.41 (0.04)	0.00 (-0.03, 0.04)	0.919	0.00 (-0.03, 0.04)	0.899
Co.Po	0.04 (0.01)	0.03 (0.01)	-0.01 (-0.02, -0.004)	0.003	-0.01 (-0.02, -0.004)	0.004
Co.Po.DM (mm)	0.145 (0.005)	0.140 (0.007)	-0.005 (-0.009, -0.001)	0.011	-0.005 (-0.009, -0.001)	0.009
BV/TV (%)	14.2 (2.4)	13.6 (2.2)	-0.5 (-2.0, 0.9)	0.407	-0.6 (-2.1, 0.9)	0.408
DISTAL TIBIA						
HRpQCT parameter	Lean (n=18) Mean (SD)	Obese (n=18) Mean (SD)	Unadjusted Mean Difference (95% CI)	P-Value	Adjusted Mean Difference (95% CI)	P-Value
D_{tot} (mg/cm^3)	235.3 (24.3)	238.5 (38.9)	3.2 (-22.1, 28.5)	0.793	2.3 (-20.5, 25.1)	0.833
$Area_{tot}$(mm^2)	916.9 (167.8)	975.9 (244.2)	59.0 (-88.3, 206.3)	0.410	66.1 (-48.3, 180.4)	0.238
D_{cort}(mg/cm^3)	652.7 (82.7)	669.4 (114.1)	16.7 (-43.3, 76.7)	0.565	14.3 (-37.2, 65.8)	0.565
$Area_{cort}$(mm^2)	48.1 (22.9)	51.4 (32.9)	3.3 (-12.9, 19.6)	0.672	2.8 (-12.1, 17.7)	0.699
Ct.Th (mm)	0.41 (0.21)	0.45 (0.35)	0.04 (-0.14, 0.23)	0.620	0.04 (-0.13, 0.21)	0.641
D_{trab}(mg/cm^3)	199.9 (30.1)	192.8 (23.5)	-7.1 (-19.9, 5.8)	0.262	-7.4 (-20.0, 5.2)	0.234
$Area_{trab}$(mm^2)	848.0 (167.4)	901.1 (255.2)	53.2 (-100.4, 206.7)	0.475	60.4 (-60.3, 181.1)	0.305
Tb.Th (mm)	0.074 (0.009)	0.065 (0.008)	-0.009 (-0.014, -0.004)	0.003	-0.009 (-0.015, -0.004)	0.002
Tb.N (mm^{-1})	2.27 (0.31)	2.50 (0.31)	0.23 (0.08, 0.38)	0.004	0.23 (0.08, 0.38)	0.006
T.S (mm)	0.38 (0.07)	0.34 (0.05)	-0.03 (-0.06, -0.01)	0.015	-0.03 (-0.06, -0.01)	0.019
Co.Po	0.055 (0.021)	0.046 (0.015)	-0.009 (-0.019, 0.002)	0.098	-0.009 (-0.019, 0.001)	0.078
Co.Po.DM (mm)	0.148 (0.007)	0.144 (0.006)	-0.004 (-0.008, -0.001)	0.012	-0.004 (-0.008, -0.001)	0.014
BV/TV (%)	16.6 (2.5)	16.1 (2.0)	-0.6 (-1.6, 0.5)	0.273	-0.6 (-1.6, 0.4)	0.243

*calculated by paired t-test

**calculated using ANCOVA

Total volumetric density (D_{tot}), total area ($Area_{tot}$), cortical density (D_{cort}), cortical area ($Area_{cort}$), cortical thickness (Ct.Th), trabecular density (D_{trab}), trabecular area ($Area_{trab}$), trabecular thickness (Tb.Th), trabecular number (Tb.N), and trabecular spacing (Tb.S), Cortical Porosity (Co.Po.), Cortical Pore Diameter (Co.Po.DM), Bone Volume/Tissue Volume (BV/TV).

Table 3: Comparison of HR-pQCT derived microFE bone strength parameters between obese and lean children matched for pubertal stage and gender calculated by paired t-tests and ANCOVA (height as a covariate in the analysis). Significance is reached at p≤0.05.

DISTAL RADIUS						
	Lean (n=18) Mean (SD)	Obese (n=18) Mean (SD)	Unadjusted Mean Difference (95% CI)	P-Value	Adjusted Mean Difference (95% CI)	P-Value
S	59.76 (10.86)	61.85 (13.67)	2.08 (-4.67, 8.83)	0.524	2.33 (-3.65, 8.32)	0.420
F.ult	3.11 (0.55)	3.19 (0.67)	0.08 (-0.25, 0.41)	0.606	0.10 (-0.20, 0.39)	0.497
(Tb.F/TF)dist	0.57 (0.08)	0.52 (0.13)	-0.05 (-0.11, 0.01)	0.107	-0.05 (-0.11, 0.01)	0.119
(Tb.F/TF)prox	0.27 (0.07)	0.24 (0.08)	-0.03 (-0.08, 0.03)	0.303	-0.03 (-0.08, 0.03)	0.315
Tb.VM	5.13 (0.40)	5.09 (0.77)	-0.04 (-0.36, 0.27)	0.770	-0.04 (-0.34, 0.27)	0.803
C.VM	8.42 (0.26)	8.45 (0.53)	0.03 (-0.25, 0.31)	0.826	0.03 (-0.25, 0.32)	0.811
BSI	14935988.51 (3097293.49)	16381259.11 (5483439.89)	1445270.60 (-1751750.36, 4642291.56)	0.354	1451903.96 (-1860144.57, 4763952.48)	0.367
DISTAL TIBIA						
	Lean (n=18) Mean (SD)	Obese (n=18) Mean (SD)	Unadjusted Mean Difference (95% CI)	P-Value	Adjusted Mean Difference (95% CI)	P-Value
S	200.16 (36.08)	205.15 (40.71)	4.99 (-14.05, 24.03)	0.587	5.85 (-9.49, 21.19)	0.431
F.ult	10.38 (1.89)	10.83 (2.15)	0.45 (-0.61, 1.52)	0.382	0.50 (-0.34, 1.34)	0.223
(Tb.F/TF)dist	0.77 (0.08)	0.75 (0.13)	-0.02 (-0.09, 0.04)	0.466	-0.02 (-0.08, 0.04)	0.473
(Tb.F/TF)prox	0.60 (0.10)	0.57 (0.14)	-0.02 (-0.10, 0.06)	0.588	-0.02 (-0.08, 0.05)	0.580
Tb.VM	5.52 (0.45)	5.21 (0.58)	-0.31 (-0.62, -0.001)	0.049	-0.31 (-0.63, 0.01)	0.058
C.VM	7.81 (0.52)	7.86 (0.61)	0.05 (-0.29, 0.40)	0.761	0.04 (-0.28, 0.36)	0.797
BSI	50468770.21 (10162836.21)	53876514.55 (12125229.19)	3407744.34 (-2628317.28, 9443805.96)	0.250	3412391.08 (-2843083.25, 9667865.41)	0.264

S- Bone stiffness (kilonewtons per millimeter); F.ult- estimated ultimate failure load (kilonewtons); (Tb.F/TF)dist – ratio of the load taken by the trabeculae in relation to the total load at the distal end; (Tb.F/TF)prox – ratio of the load taken by the trabeculae in relation to the total load at the proximal end; Tb.VM - average von Mises stresses in the trabecular bone (megapascals); C.VM - average von Mises stresses in the cortical bone (megapascals); BSI – Bone strength index (mg^2/mm^4)

Table 4: Spearman rank correlations between mass and HR-pQCT cortical and trabecular parameters at the distal radius and distal tibia. Significance is reached at p≤0.05.

	Distal Radius									
	Lean Mass		**Subtotal Fat Mass**		**Subtotal Fat Mass %**		**Truncal Fat Mass**		**Truncal Fat Mass %**	
	r (95% CI)	P-Value	r (95% CI)	P-Value	r (95% CI)	P-Value	r (95% CI)	P-Value	r (95% CI)	P-Value
Co.Po	-0.34 (-0.61, -0.03)	0.046	-0.57 (-0.75, -0.28)	<0.001	-0.57 (-0.79, -0.23)	<0.001	-0.59 (-0.77, -0.32)	<0.001	-0.58 (-0.79, -0.25)	<0.001
Co.Po.DM (mm)	-0.04 (-0.36, 0.31)	0.832	-0.38 (-0.65, -0.02)	0.024	-0.41 (-0.72, -0.03)	0.013	-0.36 (-0.63,-0.32)	0.032	-0.41 (-0.71, -0.06)	0.010
Distal Tibia										
Tb.Th (mm)	-0.31 (-0.62, 0.11)	0.064	-0.61 (-0.82, -0.30)	<0.001	-0.62 (-0.84, -0.32)	<0.001	-0.61 (-0.85, -0.25)	<0.001	-0.60 (-0.79, -0.37)	<0.001
Tb.N (mm^{-1})	0.23 (-0.14, 0.51)	0.177	0.32 (-0.01, 0.61)	0.057	0.28 (-0.08, 0.58)	0.096	0.32 (-0.04, 0.64)	0.059	0.30 (-0.07, 0.62)	0.074
Tb.S (mm)	-0.19 (-0.51, 0.20)	0.281	-0.25 (-0.59, 0.15)	0.150	-0.21 (-0.55, 0.16)	0.229	-0.24 (-0.56, 0.10)	0.158	-0.22 (-0.51, 0.07)	0.189
Co.Po.DM (mm)	-0.38 (-0.68, 0.02)	0.024	-0.32 (-0.64, 0.05)	0.056	-0.27 (-0.58, 0.11)	0.115	-0.33 (-0.60, -0.02)	0.048	-0.28 (-0.54, 0.02)	0.103
Tb.VM	-0.09 (-0.43, 0.24)	0.623	-0.35 (-0.64, -0.02)	0.037	-0.39 (-0.68, -0.03)	0.019	-0.37 (-0.62, -0.07)	0.028	-0.37 (-0.66, -0.01)	0.028

Trabecular thickness (Tb.Th), trabecular number (Tb.N), trabecular spacing (Tb.S), Cortical Porosity (Co.Po.), Cortical Pore Diameter (Co.Po.DM), Tb.VM - average von Mises stresses in the trabecular bone (megapascals)

Table 5: Comparison of biochemistry measurements between obese and lean children matched for pubertal stage and gender calculated by paired t-tests.

	Lean (n=18) Mean (SD)	Obese (n=18) Mean (SD)	Unadjusted Mean Difference (95% CI)	P-Value
Adiponectin (ng/ml)	102.87 (44.73)	95.92 (30.74)	-6.95 (-37.77, 23.86)	0.639
Leptin (pg/ml)	98.05 (75.40)	805.25 (440.63)	707.20 (496.52, 917.89)	<0.001
Oestrogen (pg/ml)	51.45 (72.50)	40.77 (64.71)	-10.67 (-49.84, 28.49)	0.572
Testosterone (ng/ml)	1.13 (2.23)	0.65 (1.10)	-0.48 (-1.27, 0.31)	0.217
Osteocalcin (ng/ml)	105.93 (37.37)	89.97 (37.70)	-15.96 (-41.92, 9.99)	0.211
Sclerostin (pg/ml)	62.40 (14.34)	65.77 (9.99)	3.38 (-6.43, 13.18)	0.476